Trapping Bragg solitons by a pair of defects

Peter Y. P. Chen,[1] Boris A. Malomed,[2,3] and Pak L. Chu[3]
[1]*School of Mechanical and Manufacturing Engineering, The University of New South Wales, Sydney 2062, Australia*
[2]*Department of Interdisciplinary Studies, Faculty of Engineering, Tel Aviv University, Tel Aviv 69978, Israel*
[3]*Optoelectronics Research Centre, Department of Electronics Engineering, City University of Hong Kong, Tat Chee Avenue, Kowloon, Hong Kong*
(Received 23 February 2005; published 8 June 2005)

We study collisions of moving solitons in a fiber Bragg grating with a structure composed of two local defects of the grating, attractive or repulsive. Results are summarized in the form of diagrams showing the share of the trapped energy as a function of the soliton's velocity and defects' strength. The moving soliton can be trapped by a *cavity* bounded by repulsive defects; a well-defined region of the most efficient trapping is identified. The trapped soliton performs persistent oscillations in the cavity, with the frequency in the GHz range. For attractive defects, essential differences are found from the earlier studied case of the collision of a soliton with a single defect: in this case, too, there appears a well-defined region of the most efficient trapping, and the largest velocity, up to which the soliton can be captured, increases. The findings may be significant for experiments aimed at the creation of "standing-light" pulses in the fiber gratings and for related applications. Collisions between identical solitons moving across the two-defect structure are also studied. On the attractive set, soliton-soliton collisions may give rise to symmetric capture of the solitons by both defects or merger into a single pulse trapped at one defect.

DOI: 10.1103/PhysRevE.71.066601 PACS number(s): 42.65.Tg, 42.79.Dj, 05.45.Yv

I. INTRODUCTION

The interaction of nontopological solitons with local defects is a topic of general interest in various physical contexts; see the review in [1] and more recent works (e.g., [2]). Recently, interactions of this type have drawn special attention in nonlinear optics, where they can be realized in terms of gap solitons (or more general wave packets [3]) in fiber Bragg gratings [4–6] or photonic crystals [7] with intrinsic defects. In particular, the collision of a moving Bragg soliton with a strongly localized attractive inhomogeneity was studied in Ref. [5]. Inhomogeneity was realized as a local disruption of the grating. A repulsive defect is also possible in the grating in the form of a short segment with enhanced Bragg reflectivity. On the basis of systematic simulations, it was concluded that three qualitatively different outcomes of the collision occur: transmission, capture, and splitting of the soliton into three pulses (transmitted, trapped, and reflected ones). In some cases (when the incident soliton is "heavy" and, strictly speaking, unstable by itself) almost all the energy goes into the reflected pulse, so that the attractive defect may look as an effectively repulsive one.

The possibility of capturing the moving soliton by the defect, and thus the formation of a stable pulse of standing light, is an issue of considerable applied interest, as it may be used to design all-optical memory elements, with the soliton playing the role of a bit. This issue is also closely related to the challenging problem of the creation of "slow light" [8] (the latter problem was specially considered in terms of slow solitons in Refs. [5,9–11]). Another potentially promising aspect of the interaction between moving solitons and grating inhomogeneities is a possibility to use it in fiber-grating sensors, which is a very important application [12] (currently, sensors operate only in the linear regime). Besides that, the interaction of moving Bragg solitons with defects is an issue of considerable interest to the general theory of solitary waves in inhomogeneous media.

The subject of this work is interaction of Bragg solitons with a symmetric pair of local defects in the fiber grating, with the distance between them on the order of several soliton's widths. We demonstrate that this setting offers new possibilities to achieve the capture of moving solitons. First, if both defects are attractive ones, the incident soliton may be slowed down and/or distorted by the first defect so as to help the second defect trap it. Achieving more efficient capture is a relevant issue, as the slowest Bragg solitons currently available to the experiment have velocity no smaller than 0.5 the maximum velocity $c_{\max}$ [13], while the largest velocity which admits the capture of the soliton by a single attractive defect of the grating is $\approx 0.45 c_{\max}$ (and in that limit, the quality of the capture is poor, as a considerable part of the soliton's energy is lost [5]). The use of the two-defect configuration may help to bridge the remaining gap between the available and necessary velocities.

Completely new possibilities are offered by a configuration consisting of two *repulsive* defects. This structure also may trap a passing soliton and then hold in the form of an oscillator in the effective *cavity* bounded by the defects. Note that the strength of the localized attractive defect, which relies upon local suppression of the Bragg reflectivity in a narrow segment of the fiber, which must be much smaller than the size of the soliton (the latter takes values in the range between ~ 1 mm and ~ 1 cm) is fundamentally limited. Contrary to this, the repulsive defect, which makes use of *locally enhanced* reflectivity, may be, in principle, arbitrarily strong [5] (see details below); hence, the repulsive pair may provide for a stronger tool for manipulations with the solitons. In addition, the gap-soliton oscillator realized in the cavity may by itself be of interest to applications, such as the development of sources or detectors of GHz radiation

(the frequency of oscillations of the Bragg soliton trapped in the cavity is expected to be in the range of 1–10 GHz).

This paper is organized as follows: the model is formulated in Sec. II. Section III presents results of a systematic numerical analysis of collisions of a free soliton with the pair of attractive defects, with the focus on possibilities to trap the soliton. Section IV deals with the most interesting case—i.e., the capture of an incident soliton by a cavity formed between two repulsive defects. In Sec. V we consider, in a less systematic form, collisions between two Bragg solitons, traveling in opposite directions, in the presence of the pair of attractive defects (the same case with the repulsive pair does not yield noteworthy results). Collisions between Bragg solitons is an issue of considerable interest [14], especially as concerns a possibility of their fusion into a single pulse [10]. In this work, we demonstrate that the pair of attractive defects may catalyze the fusion, ending up with a single soliton trapped by one of the defects. The paper is concluded by Sec. VI.

II. MODEL

We approximate a local disruption (or enhancement) of the resonant Bragg grating (the defect) by δ-function terms added to the standard system [15,16] of coupled-mode equations for the amplitudes of right- and left-traveling waves, $u(x,t)$ and $v(x,t)$, in the nonlinear fiber equipped with Bragg grating. Thus we arrive at the following model, written in the usual notation [15,16]:

$$i\frac{\partial u}{\partial t}+i\frac{\partial u}{\partial x}+v+\left(\frac{|u|^2}{2}+|v|^2\right)u=\kappa\left[\delta\left(x-\frac{L}{2}\right)+\delta\left(x+\frac{L}{2}\right)\right]v, \tag{1}$$

$$i\frac{\partial v}{\partial t}-i\frac{\partial v}{\partial x}+u+\left(\frac{|v|^2}{2}+|u|^2\right)v=\kappa\left[\delta\left(x-\frac{L}{2}\right)+\delta\left(x+\frac{L}{2}\right)\right]u, \tag{2}$$

where x is the coordinate along the fiber, t is time, and the ordinary ratio between the self-phase-modulation (SPM) and cross-phase-modulation (XPM) coefficients, 1:2, is adopted. In these equations, the SPM coefficient itself, group velocities, and Bragg reflectivity in the uniform grating are all normalized to be 1, and two identical pointlike defects are placed at points $x=\pm L/2$. The model does not include a possible but less interesting additional component of the defect, in the form of a local perturbation of the refractive index [4,5].

While Eqs. (1) and (2) describe temporal solitons, the same model may also be realized in the spatial domain. In that case, it describes two waves in a nonlinear planar waveguide, with t replaced by the propagation distance and x being the transverse coordinate. The Bragg reflection is provided by a grating in the form of a system of parallel ridges or grooves with spacing h on the surface of the waveguide, the Poynting vectors of the two waves forming angles $\pm\theta$ with the grating. This setting may give rise to *spatial gap solitons* [17] under the Bragg resonant-reflection condition $\lambda=(2h/n)\sin\theta$, where λ is the wavelength and $n=1,2,\ldots$ is the order of the resonance (in the limiting case of $\theta=\pi/2$, this condition carries over into the one for the fiber grating, $h=\lambda n/2$). Recently, discrete spatial gap solitons were created experimentally in an array of tunnel-coupled waveguides with a strong nonlinearity [18].

The real (positive or negative) constant κ in Eqs. (1) and (2) measures the strength of the local defects, which may be created as narrow regions with suppressed ($\kappa>0$) or enhanced ($\kappa<0$) grating. In either case, the size of the perturbed regions is assumed to be much smaller than a characteristic length $x_{\rm refl}$ necessary for the complete reflection on the uniform grating, which is, typically, $\sim$1 mm in physical units [13,16], or may be increased up to $\sim$1 cm for very weak gratings. The same length $x_{\rm refl}$ determines a characteristic spatial width of the soliton. For positive κ, this implies that the δ-function terms in Eqs. (1) and (2) correctly describe the narrow grating-suppression defects only with $\kappa \ll 1$, as the Bragg reflectivity in the uniform grating is normalized to be 1, which implies $x_{\rm refl}\sim 1$ in the same units. Consideration of the form of the soliton solution [see Eqs. (6) and (7) below] and detailed results of numerical simulations, it is reasonable to fix the applicability condition of the present model, for positive κ, as

$$\kappa \leqslant 0.3. \tag{3}$$

On the other hand, for negative κ, there is no principal limit on the size of $|\kappa|$, as in this case the δ-function terms in Eqs. (1) and (2) account for the local perturbation in the form of enhanced Bragg reflection. As the gratings used in experiments with the Bragg solitons are rather weak ("shallow") [13], the local enhancement may be (relatively) strong [5] (although the form of the coupled-mode equations may need to be altered for deep gratings [19]).

Equations (1) and (2) can be derived from the Hamiltonian

$$H=\int_{-\infty}^{+\infty}\left[\frac{1}{2}i(-u^*u_x+v^*v_x+uu_x^*-vv_x^*)-\frac{1}{4}(|u|^4+|v|^4)-|u|^2|v|^2-(u^*v+uv^*)\right]dx+H_{\rm int}, \tag{4}$$

with the asterisk and subscript standing for the complex conjugation and partial derivative, respectively. The perturbation part of the Hamiltonian, which accounts for the interaction of the soliton with the defects, is

$$H_{\rm int}=\sum_{+,-}\kappa(u^*v+uv^*)|_{x=\pm L/2}. \tag{5}$$

Exact solutions to Eqs. (1) and (2) with $\kappa=0$, which describe solitons moving at a velocity $c(c^2<1)$ in the uniform fiber grating, were found in Refs. [15]:

$$u_{\rm sol}=\sqrt{\frac{2(1+c)}{3-c^2}}(1-c^2)^{1/4}W(X)\exp[i\phi(X)-iT\cos\theta],$$

$$v_{\rm sol} = -\sqrt{\frac{2(1-c)}{3-c^2}}(1-c^2)^{1/4}W^*(X)\exp[i\phi(X) - iT\cos\theta]. \tag{6}$$

Here, θ is an intrinsic parameter of the soliton family which takes values $0<\theta<\pi$ and

$$X = \frac{x-\xi(t)}{\sqrt{1-c^2}}, \quad T = \frac{t-cx}{\sqrt{1-c^2}},$$

$$\phi(X) = \frac{4c}{3-c^2}\tan^{-1}\left\{\tanh[(\sin\theta)X]\tan\left(\frac{\theta}{2}\right)\right\},$$

$$W(X) = (\sin\theta)\,\mathrm{sech}\left[(\sin\theta)X - \frac{i\theta}{2}\right], \tag{7}$$

with $d\xi/dt=c$. It is known that this family of Bragg solitons is stable in the region of $\theta\leqslant\theta_{\rm cr}$, with $\theta_{\rm cr}$ slightly larger than $\pi/2$ [in particular, $\theta_{\rm cr}\approx 1.01(\pi/2)$ for $c=0$ [20,21]]. The critical value $\theta_{\rm cr}$ very weakly depends on c, up to $|c|=1$ [21].

Equations (1) and (2) with $\kappa\neq 0$ conserve two dynamical invariants: the Hamiltonian (4) and the norm of the solution (the latter is frequently called *energy* in optics, although it is different from the Hamiltonian),

$$E \equiv \int_{-\infty}^{-\infty}(|u|^2+|v|^2)dx. \tag{8}$$

The norm of the exact solution (6) (for $\kappa=0$) is

$$E_{\rm sol} \equiv \frac{8\theta(1-c^2)}{3-c^2}. \tag{9}$$

An exact solution is also available for a quiescent ($c=0$) soliton trapped by a single defect with the strength κ (of either sign), set at $x=0$ [5]:

$$\{u,v\} = \pm\sqrt{\frac{2}{3}}e^{-it\cos\theta}(\sin\theta)\,\mathrm{sech}\left[(x+a\,\mathrm{sgn}\,x)\sin\theta \mp \frac{i\theta}{2}\right], \tag{10}$$

where the two signs pertain to the u and v components, and the constant a is uniquely determined by the relation

$$\tanh(a\sin\theta) = \frac{\tanh(\kappa/2)}{\tan(\theta/2)}. \tag{11}$$

The pinned-soliton solution exists in the region

$$2\tan^{-1}[\tanh(\kappa/2)] < \theta < \pi. \tag{12}$$

Its energy (norm), defined as per Eq. (8), is

$$E = \frac{8}{3}\left(\theta - \left[\frac{\pi}{2} - \sin^{-1}(\mathrm{sech}\,\kappa)\right]\mathrm{sgn}\,\kappa\right) \tag{13}$$

[cf. Eq. (9) with $c=0$], and its intensity at the central point is

$$|u(x=0)|^2 = |v(x=0)|^2 = \frac{2}{3}\frac{\sin^2\theta}{\sinh^2(a\sin\theta)+\cos^2\theta} \tag{14}$$

[for the soliton pinned at the repulsive defect, with $\kappa<0$, Eq. (11) yields $a<0$; hence, this soliton has a local minimum, rather than maximum, at $x=0$]. The pinned solitons were found to be stable only if θ is very close to $\pi/2$ (and only for $\kappa>0$); note that $\theta=\pi/2$ always belongs to the existence interval (12), and Eq. (11) yields $a=\kappa/2$ for $\theta=\pi/2$.

If κ is a small parameter, the interaction between a slow soliton (6), with $|c|\ll 1$, and the pointlike defect is governed by an effective potential which is calculated by substitution of the wave form (6) in the interaction Hamiltonian (5) [5],

$$U_{\rm int}(\xi) = -\frac{8}{3}\frac{\kappa\sin^2\theta}{\cosh(2\xi\sin\theta)+\cos\theta}, \tag{15}$$

where ξ is the instantaneous coordinate of the soliton's center. The slow soliton moves in this potential as a nonrelativistic particle with effective mass $M(\theta)=(8/9)(7\sin\theta - 4\theta\cos\theta)$ [11]. In the model with two defects, an effective potential can be constructed as a superposition of two singe-defect potentials (15), $U_{\rm eff}(\xi)=U_{\rm int}(\xi-L/2)+U_{\rm int}(\xi+L/2)$.

III. INTERACTION OF A FREE SOLITON WITH THE PAIR OF ATTRACTIVE DEFECTS

We start the analysis with the case of two attractive defects, which is an extension of the previously developed analysis of the interaction of the soliton with a single defect [4,5]. With either sign of the defects, Eqs. (1) and (2) were simulated in the domain $-60<x<+60$ by means of the standard split-step scheme. The spatial derivatives were computed through the fast Fourier transform on the mesh of 1024 points. A typical width of the soliton being ~ 1.5 [in normalized units adopted in Eqs. (1) and (2)], this implies that the soliton's shape was approximated by a set of $\simeq 30$ points. It was checked that a finer mesh produced the same results. The δ functions were modeled in the usual way, by a rectangular-box inhomogeneity including, in most cases, four points. We checked that a more accurate approximation for the δ functions did not affect the results.

The time derivative was approximated by the forward finite difference. The respective step size Δt was taken smaller and smaller until results became insensitive to its further reduction. In some cases, it was necessary to use Δt as small as 5×10^{-4}. To prevent emitted radiation from getting back into the integration domain, two edge absorbers were installed, each occupying 20 points of the discrete mesh (it was observed that, in very long simulations, the absorbers were essential, really suppressing the emitted radiation).

Below, results are displayed for the pair of defects placed at points $x=\pm 8$, so that the distance $L=16$ between them is, roughly, 10 times the mean soliton's width. Results obtained with other values of L are very similar to those reported here.

Simulations started with the exact soliton (6), taken sufficiently far from (to the right of) the defects; see Fig. 1. To initiate the collision, the soliton was lent a negative velocity c (therefore its u and v components are not symmetric in Fig. 1). It was checked that setting the initial soliton still farther from the defects did not affect the outcome of the collision.

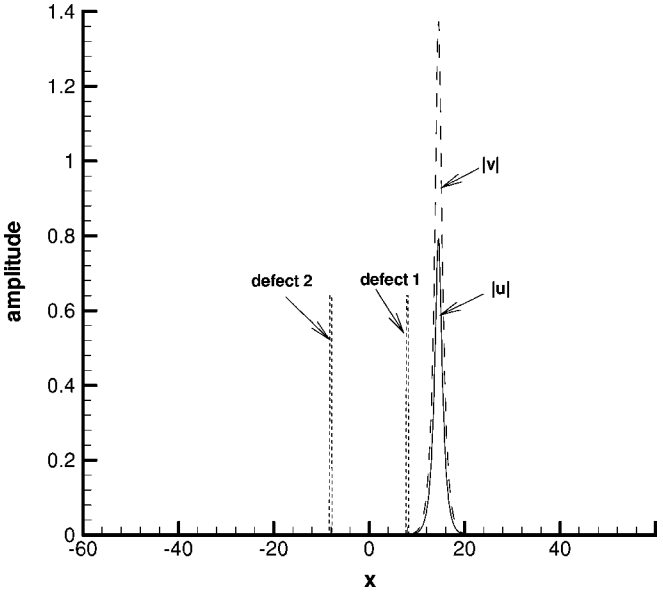

FIG. 1. The initial configuration used in the simulations. Here, the soliton is shown with $\theta=\pi/2$ and $c=-0.5$; see Eqs. (6).

Most results are displayed below for the value $\theta=\pi/2$ of the intrinsic parameter of the soliton; see Eqs. (7). This choice is quite natural, as the soliton's width $\sim 1/\sin\theta$ attains its minimum in this case; hence, it is of major interest to the experiment and potential applications. Note that a soliton trapped by the single attractive defect may be stable only for θ very close to $\pi/2$ [5], and this value simultaneously belongs to the stability region of the free Bragg solitons [20,21]. However, some results will also be given for values of θ essentially different from $\pi/2$.

If the first attractive defect fails to capture the incident soliton, this defect, nevertheless, affects the soliton in such a way (the soliton undergoes an internal distortion, and in some cases it is also slowed down) that its capture by the second defect is facilitated. An example of such an *assisted capture* of a relatively slow soliton by the second defect is given in Fig. 2(a). In the same setting, a faster soliton splits, as shown in Fig. 2(b), with a considerable part of its energy trapped by the second defect, while another part escapes in the form of a weak transmitted pulse. A very small share of the energy is reflected, by both defects, in the form of radiation waves. A common noteworthy feature of the examples showed in Figs. 2(a) and 2(b) is a possibility to capture the entire soliton or its large part by the second defect in cases when the single attractive defect would fail in doing this.

Results of many runs of simulations are summarized in the diagram displayed in Fig. 3(a) which shows the share of the initial soliton's energy [see Eq. (8)] eventually trapped by the second attractive defect. As is seen, there is a well-defined parameter region providing for the most efficient capture. This conclusion is additionally illustrated by cross sections of the diagram at two different fixed values of the velocity, which are displayed in Fig. 3(b). If the value of κ is smaller than one providing for essential trapping at a given c, the soliton passes through the two-defect trap (in particular, a sharp border of the capture region for $|c|=0.4$ starts at $\kappa \approx 0.25$, which is very close to the minimum value of κ providing for the capture of the soliton at the same velocity by the single defect [5]). In the opposite case, if κ exceeds values providing for the capture, the soliton actually does not reach the second defect as it gets either trapped (and sometimes destroyed) by the first defect or bounces back from it (recall that, in some cases, a bounce from the attractive defect is possible [5]).

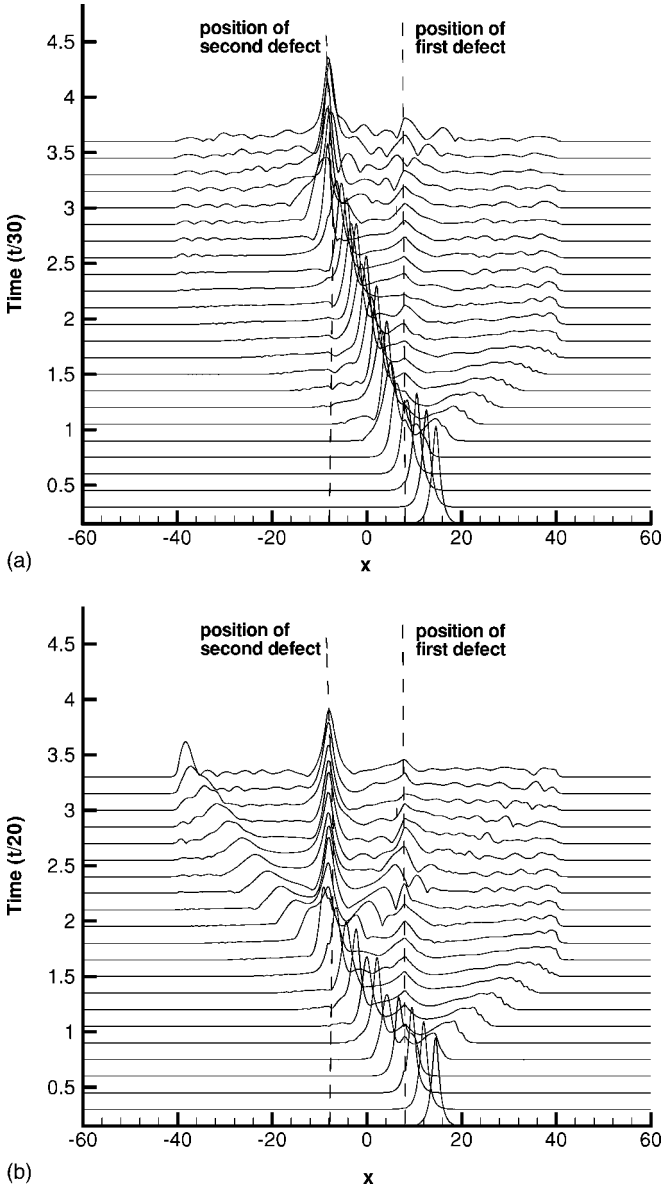

FIG. 2. Typical examples of the interaction of a moving Bragg soliton with the attractive two-defect structure: (a) The soliton with the velocity $c=-0.4$ passes the first defect, but is easily captured by the second one, both with having the strength $\kappa=0.27$. The soliton's intrinsic parameter is $\theta=\pi/2$. (b) A large part of the energy of the incident soliton with $c=-0.5$ and $\theta=\pi/2$ (which would freely pass the single defect) is snared by the second defect, in the case of $\kappa=0.3$.

It is relevant to compare these results to those obtained with a single attractive defect. For this purpose, Fig. 3(c) shows the capture diagram for that case. As is seen, the character of the capture is then completely different, as there is

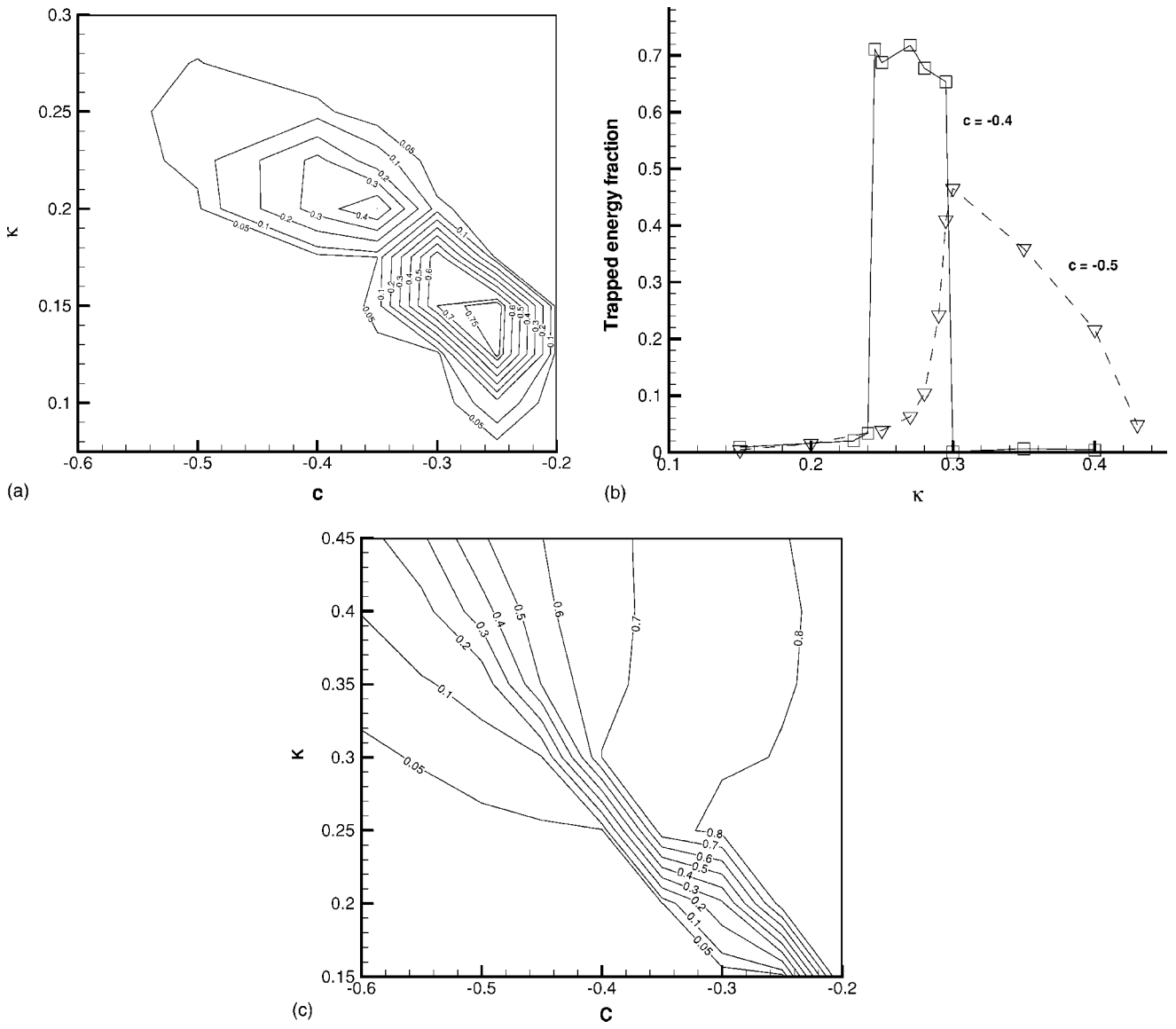

FIG. 3. (a) The contour plots of the share of the initial soliton's energy trapped by the second defect as a result of the collision in the plane of the soliton's velocity c and defects' strength κ (for the attractive defects, with $\kappa>0$). The diagram pertains to the solitons with $\theta=\pi/2$. (b) Cross sections of the diagram from panel (a) at fixed values of the velocity. (c) For comparison with panel (a), the contour plots of the trapped-energy share is shown here for the single-defect model. This diagram also pertains to the solitons with $\theta=\pi/2$.

no distinguished region providing for the most efficient trapping, in contrast with the two-defect model. Taking into regard the limitation (3) on the size of positive κ, we conclude that, at the smallest velocity available to the current experiments [13], $|c|=0.5$, the set of single attractive defects admits the capture of only $\simeq 7\%$ of the soliton's energy, while the two-defect set captures 40% (counting only what is captured by the second defect). Thus, the set consisting of two attractive defects helps to snare a moving soliton in a more efficient way than a single defect can do it; however, the efficacy of the capture is still below 50%. Below, it will be shown that the set of two repulsive defects provides for higher efficacy.

All the above results pertain to $\theta=\pi/2$, which corresponds, as said above, to the narrowest soliton. Results were also collected for other values of θ; see an example in Fig. 4 for $\theta=\pi/4$ (the shape of this soliton is closer to the nonlinear-Schrödinger limit [14]). As is seen from Fig. 4(a), a region of the strongest trapping can be also identified for the solitons with smaller θ, although it is shifted to much smaller velocity.

IV. TRAPPING OF SOLITONS BY A PAIR OF REPULSIVE DEFECTS

As explained above, the possibility to capture a moving Bragg soliton in the cavity formed by two repulsive defects is a new effect, without any previously considered counterpart. A typical example of the capture of the soliton into a stable state, in the form of a stable pulse performing persistent oscillations in the cavity, is displayed in Fig. 5. The evolution of the pulse's energy, which we define as the share

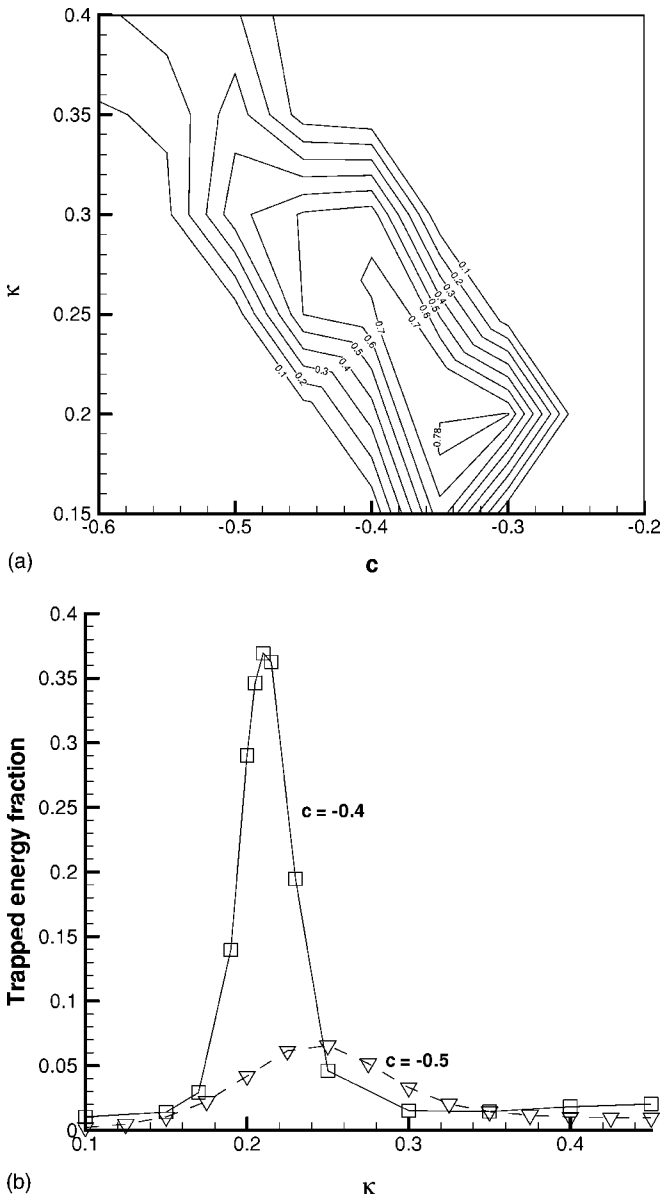

FIG. 4. The same as in Fig. 3 but for the soliton with $\theta=\pi/4$. (a) Contour plots for the trapped energy. (b) Cross sections of the diagram in panel (a) at fixed values of the velocity.

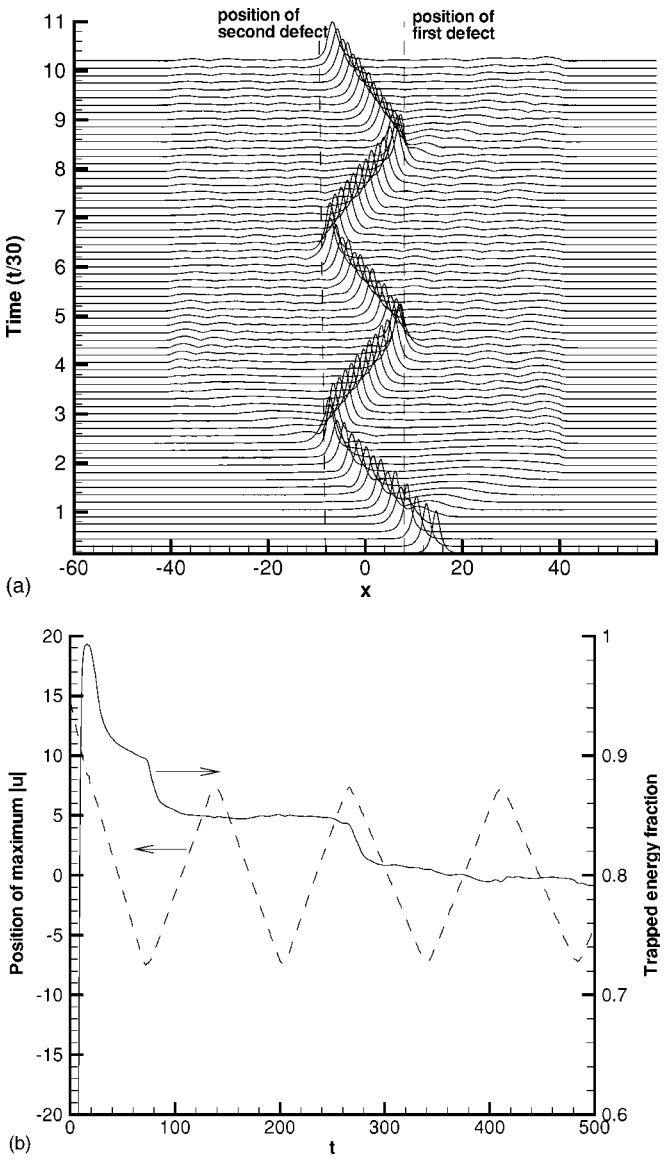

FIG. 5. Capture of the soliton (with $\theta=\pi/2$), moving at the velocity $c=0.4$, by the pair of repulsive defects with the strength $\kappa=-0.2$. (a) The evolution of the field $|u(x,t)|^2$. (b) The trajectory of the center of the captured soliton (dashed curve) and evolution of the share ("fraction") of the initial energy which is trapped between the defects (solid curve). The soliton's center is realized as a point where the field $|u(x)|$ attains its maximum, at a given moment of time.

of the initial energy of the soliton confined in the cavity (between the points $x=\pm L/2$), shows a trend to stabilization [see Fig. 5(b)] after the captured soliton suffers some radiation loss at a transient stage (small portions of radiation are emitted when the soliton bounces from the defects which bound the cavity).

An overall diagram showing the efficiency of the soliton's capture by the set of two repulsive defects is displayed in Fig. 6(a), and examples of its cross sections at fixed values of the velocity are shown in Fig. 6(b). If the defects' strength $|\kappa|$ is smaller than the minimum one which is necessary for the capture, the soliton passes through the cavity; in the opposite case, when $|\kappa|$ exceeds the maximum value admitting the capture, the soliton bounces back from the first defect.

These capture diagrams resemble their counterparts in the case of the attractive set (cf. Fig. 3) in the sense that a region of the most efficient capture can again be clearly identified. However, a notable difference is that, in comparison with the case of the two attractive defects, the efficient region extends to larger values of c. In particular, Fig. 6(b) shows that the trapping efficacy of 60% can be attained for $|c|=0.5$, which is definitely beyond the reach of the settings with attractive defects.

The set of repulsive defects is quite efficient too in trapping "heavy" solitons, with $\theta>\pi/2$. Strictly speaking, such solitons are unstable [20,21], but if the evolution time between the creation of the soliton and its collision with the defect structure is not too large, the consideration of their

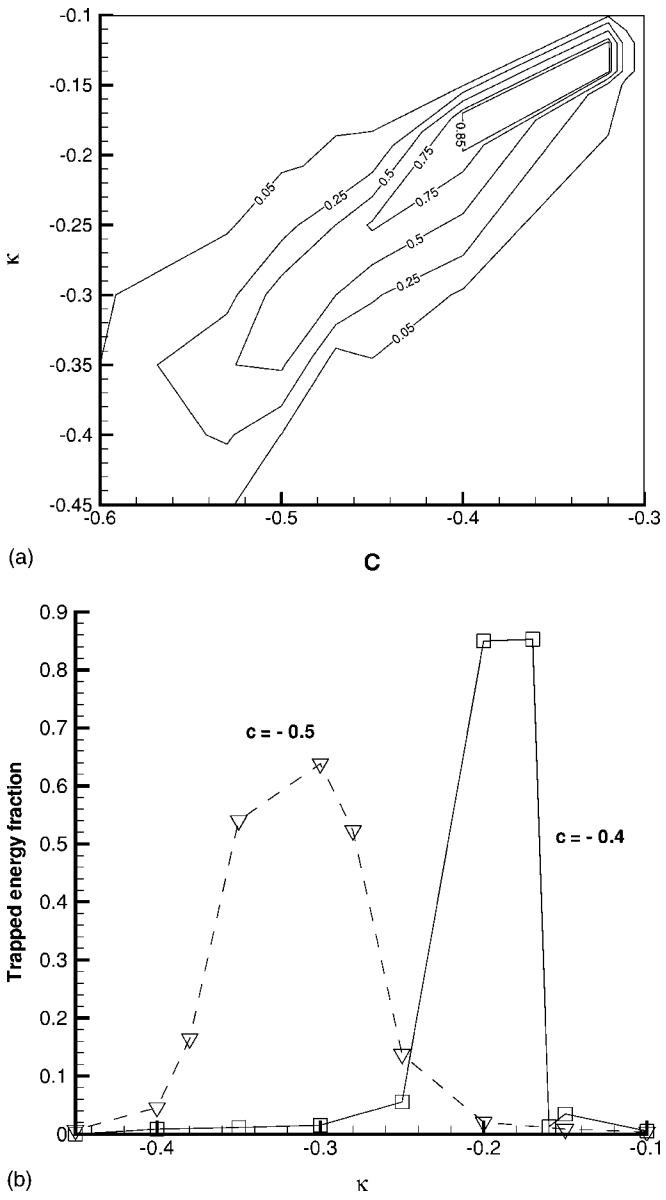

FIG. 6. Capture of the moving solitons (with $\theta=\pi/2$) by a set of two identical repulsive defects. (a) Contour plots of the share of the initial energy that remains trapped in the cavity between the defects; cf. Fig. 3(a). (b) Cross sections of the diagram in panel (a) at two fixed values of the velocity; cf. Fig. 3(b).

evolution also makes sense. We have observed that such solitons are readily captured by the pair of repulsive defects, and they gradually reduce their energy (in other words, the value of θ) in the course of the oscillatory motion in the cavity, as shown in Fig. 7. Although very long simulations were not run in this case, we expect that the soliton will eventually relax to one with a quasistationary shape. The simulations also showed that "light" solitons (for instance, one with $\theta=\pi/4$) are easily trapped by the repulsive set too and then perform oscillations in the cavity without any conspicuous loss (not shown here). Thus, the trapping mode provided by the repulsive set is quite robust, providing for the capture of a broad spectrum of the Bragg solitons.

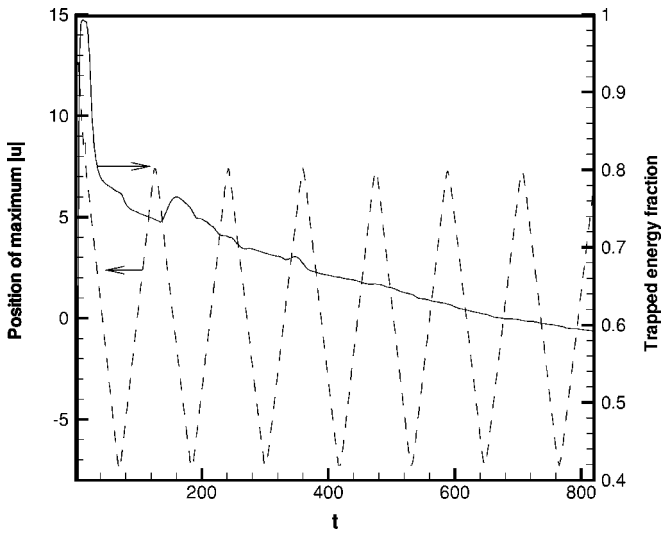

FIG. 7. Oscillations of a "heavy" soliton, with $\theta=(3/4)\pi$ and $c=-0.5$, captured by the pair of repulsive defects with $\kappa=-0.35$. The drop in the share of the energy trapped in the cavity is explained by radiation loss.

V. COLLISIONS OF SOLITONS IN THE TWO-DEFECT STRUCTURE

A natural extension of the above analysis is to consider collisions between two identical in-phase solitons (with zero phase shift between them) moving in opposite directions, so that the collision point falls within the space between the two defects. Collisions of solitons in the presence of a single attractive defect were simulated in Ref. [5], with a conclusion that the collision does not essentially facilitate the capture of a pulse by the defect. In the case of two attractive defects the situation may be different, with sundry outcomes of the collision. One possibility is that each soliton gets captured by a defect, so that a symmetric trapped pair of the solitons appears; see an example in Fig. 8(a). Another noteworthy outcome is a possibility of *spontaneous symmetry breaking*, resulting in a *merger* of the colliding solitons into a single one, which collects nearly all the initial energy. This single pulse may be trapped by either defect; see Fig. 8(b).

The latter outcome can be readily explained. Indeed, identical solitons with zero phase shift attract each other; hence, the collision between them leads to the formation of a temporary "lump" (single pulse), as seen in both panels 8(a) and 8(b). In the former case, the lump splits again into two quasisolitons, and each is then captured by one of the attractive defects. However, in the latter case the lump stays unsplit for a longer time (because the collision took place with smaller velocities $c=\pm 0.4$, rather than $c=\pm 0.5$). This heavy pulse is attracted by both defects, and obviously, its equilibrium position at the midpoint is unstable. Therefore, a small shift of the lump from the center leads to its capture by a single defect. Although no off-center shift was deliberately introduced in the simulations, numerical errors may provide for a small perturbation that initiates the spontaneous symmetry breaking.

Thus, the pair of attractive defects gives rise to the collisional dynamics which may be drastically different from

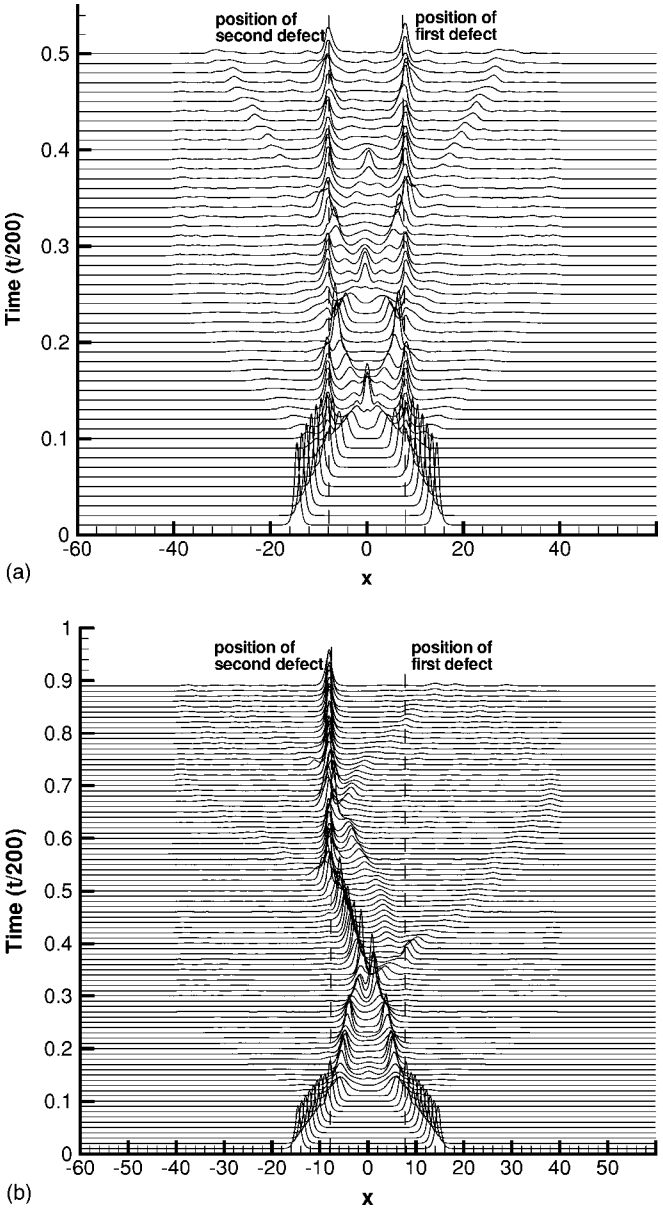

FIG. 8. Outcomes of collisions between two identical solitons with $\theta=\pi/2$ and zero phase difference, the collision point being set at the middle of the pair of attractive defects. (a) Formation of a symmetric trapped state of two solitons in the case when they collide with velocities $c=\pm 0.5$ and the defects' strength is $\kappa=0.45$. (b) Merger of two solitons, colliding with velocities $c=\pm 0.4$, into a single trapped one. In this case, the strength of the defects is $\kappa=0.295$.

what was observed in the presence of a single attractive defect. Unlike the attractive set, a pair of repulsive defects does not generate particularly interesting results of the collision. Typically, the solitons either bounce and separate or pass through each other (provided that they are given zero phase difference, so that their mutual interaction is attractive).

VI. CONCLUSION

We have investigated interactions of moving Bragg solitons with a structure composed of two defects, attractive or repulsive. Results of the collisions were quantified by parametric diagrams which show the share of the trapped energy as a function of the soliton's velocity and strength of the defects. In the case of the attraction, essential differences from the earlier studied case [5] of the collision of a soliton with a single defect were observed: there appears a well-defined region of the most efficient trapping, and the maximum velocity, up to which the capture of a considerable part of the soliton's energy is possible, increases.

A totally new situation is the capture of the moving soliton by a cavity bounded by two repulsive defects. In this case, the trapped soliton then performs persistent oscillations in the cavity (with the frequency in the GHz range) and may find specific applications in this capacity. A parametric region of the most efficient capture was identified in this case too. A promising result is that the region of the efficient capture extends to values of the velocity which are available in current experiments. A moving unstable ("too heavy") soliton can also be readily captured by the cavity and reshaped into a stable oscillating pulse.

These results may be relevant to experiments aimed at the creation of pulses of "standing light" in fiber gratings, as well as for potential applications to the design of soliton-based optical sensors, and of all-optical memory cells, where solitons would be used as bits.

Finally, we have considered collisions between identical in-phase solitons in the presence of the two-defect structure. It was concluded that, with the attractive defects, nontrivial outcomes are possible: namely, symmetric capture of two solitons by the two defects and, what is especially interesting, merger of the solitons into a single pulse captured by one defect.

ACKNOWLEDGMENTS

Two authors (P.Y.P.C. and B.A.M.) appreciate hospitality of the Optoelectronics Research Centre at the Department of Electronic Engineering, City University of Hong Kong.

[1] Y. S. Kivshar and B. A. Malomed, Rev. Mod. Phys. **61**, 763 (1989).

[2] K. Forinash, M. Peyrard, and B. Malomed, Phys. Rev. E **49**, 3400 (1994); S. A. Kiselev, S. R. Bickham, and A. J. Sievers, Phys. Rev. B **50**, 9135 (1994); X. D. Cao and B. A. Malomed, Phys. Lett. A **206**, 177 (1995); S. Rakhmanova and D. L. Mills, Phys. Rev. B **58**, 11458 (1998); N. V. Alexeeva, I. V. Barashenkov, and G. P. Tsironis, Phys. Rev. Lett. **84**, 3053 (2000); R. H. Goodman, P. J. Holmes, and M. I. Weinstein, Physica D **192**, 215 (2004).

[3] C. M. de Sterke, E. N. Tsoy, and J. E. Sipe, Opt. Lett. **27**, 485 (2002).

[4] R. H. Goodman, R. E. Slusher, and M. I. Weinstein, J. Opt. Soc. Am. B **19**, 1635 (2002).
[5] W. C. K. Mak, B. A. Malomed, and P. L. Chu, J. Opt. Soc. Am. B **20**, 725 (2003).
[6] W. C. K. Mak, B. A. Malomed, and P. L. Chu, Phys. Rev. E **67**, 026608 (2003).
[7] B. I. Mantsyzov, I. V. Mel'nikov, and J. S. Aitchison, Phys. Rev. E **69**, 055602 (2004); IEEE J. Sel. Top. Quantum Electron. **10**, 893 (2004).
[8] J. Marangos, Nature (London) **397**, 559 (1999); K. T. McDonald, Am. J. Phys. **68**, 293 (2000).
[9] J. E. Heebner, R. W. Boyd, and Q. H. Park, Phys. Rev. E **65**, 036619 (2002).
[10] W. C. K. Mak, B. A. Malomed, and P. L. Chu, Phys. Rev. E **68**, 026609 (2003).
[11] W. C. K. Mak, B. A. Malomed, and P. L. Chu, J. Mod. Opt. **51**, 2141 (2004).
[12] J. M. Senior, S. E. Moss, and S. D. Cusworth, Fiber Integr. Opt. **17**, 3 (1998); Y. J. Rao, Opt. Lasers Eng. **31**, 297 (1999).
[13] B. J. Eggleton, R. E. Slusher, C. M. de Sterke, P. A. Krug, and J. E. Sipe, Phys. Rev. Lett. **76**, 1627 (1996); C. M. de Sterke, B. J. Eggleton, and P. A. Krug, J. Lightwave Technol. **15**, 1494 (1997).
[14] N. M. Litchinitser, B. J. Eggleton, C. M. de Sterke, A. B. Aceves, and G. P. Agrawal, J. Opt. Soc. Am. B **16**, 18 (1999).
[15] A. B. Aceves and S. Wabnitz, Phys. Lett. A **141**, 37 (1989); D. N. Christodoulides and R. I. Joseph, Phys. Rev. Lett. **62**, 1746 (1989).
[16] C. M. de Sterke and J. E. Sipe, Prog. Opt. **33**, 203 (1994).
[17] J. Feng, Opt. Lett. **18**, 1302 (1993); R. F. Nabiev, P. Yeh, and D. Botez, *ibid.* **18**, 1612 (1993).
[18] D. Mandelik, R. Morandotti, J. S. Aitchison, and Y. Silberberg, Phys. Rev. Lett. **92**, 093904 (2004).
[19] T. Iizuka and C. M. de Sterke, Phys. Rev. E **61**, 4491 (2000).
[20] B. A. Malomed and R. S. Tasgal, Phys. Rev. E **49**, 5787 (1994).
[21] I. V. Barashenkov, D. E. Pelinovsky, and E. V. Zemlyanaya, Phys. Rev. Lett. **80**, 5117 (1998).